Biophysical Journal
Article

Biophysical Society

Hyaluronan Disrupts Cardiomyocyte Organization within 3D Fibrin-Based Hydrogels

Nesrine Bouhrira,[1] Peter A. Galie,[1,*] and Paul A. Janmey[2]
[1]Department of Biomedical Engineering, Rowan University, Glassboro, New Jersey and [2]Department of Physiology, University of Pennsylvania, Philadelphia, Pennsylvania

ABSTRACT The extracellular matrix in vivo contains variable but often large amounts of glycosaminoglycans that influence cell and tissue function. Hyaluronan (HA) is an abundant glycosaminoglycan within the extracellular matrix of the myocardium during early development and in the aftermath of a myocardial infarction. Its flexible anionic structure has a strong influence on mechanical response and interstitial fluid flow within the matrix. Additionally, HA has a direct, biochemical effect on cells through an array of cell-surface receptors, including CD44, RHAMM/CD168, and other surface-exposed structures. Recent studies have shown that HA modulates the response of cardiomyocytes and other cell types to two-dimensional substrates of varying elastic moduli. This study investigates the force response to HA of cardiomyocytes and cardiac fibroblasts within three-dimensional matrices of variable composition and mechanical properties in vitro. HA significantly decreased the force exerted by the cell-matrix constructs in a tensiometer testing platform and within microfabricated tissue gauges. However, its effect was no different from that of alginate, an anionic polysaccharide with the same charge density but no specific transmembrane receptors. Therefore, these results establish that HA exerts a generic physical-chemical effect within three-dimensional hydrogels that must be accounted for when interrogating cell-matrix interactions.

INTRODUCTION

Recent studies have elucidated the role of environmental factors in modifying the cellular response to the mechanics of its substrate. Normally, cells on stiff substrates exert higher traction forces and spread to larger areas by processes mediated by established signaling pathway, including Rho/ROCK (1–3), MAP kinases (4,5), and YAP/TAZ (6–8). However, there are multiple examples of this response being altered by the presence of other stimuli. Both shear stress and cyclic strain have the ability to induce the spreading of cells on soft substrates (9,10). Stiffness sensing, at least in some cell types, is not mimicked by changes in the density of adhesion proteins or the integrins to which they bind (11,12), but it can be modified by some biochemical stimuli, as exemplified by a study showing that cardiomyocytes plated on the surface of cross-linked hyaluronan (HA) behaved as if the substrates had an elastic modulus that was an order of magnitude greater than its actual value (13). The cells developed augmented sarcomeric structures in a process mimicking hypertrophy in the myocardium. This study extends the investigation of HA's mechano-modulating effect by using three-dimensional (3D) constructs to more closely mimic the in vivo microenvironment and determine its role within the myocardium.

HA is an anionic, linear polysaccharide found in the extracellular matrix (ECM) of multiple soft tissues, including the myocardium (14). Its high negative charge derives from its D-glucuronic acid groups (15). HA binds other ECM components, including fibronectin (16). Its stability in the ECM, combined with its high charge density exerts a substantial effect on fluid transport within tissues. In addition to its matrix-related effects, HA also binds to a wide array of cell-surface receptors, including CD44 (17), RHAMM/CD168 (18), and ICAM-1 (19). It is also a critical component of the glycocalyx. A primary goal of this study is to resolve both the matrix mechanics and cell-mediated effects using 3D cocultures of cardiomyocytes and cardiac fibroblasts.

HA is an important component of the myocardial ECM, primarily during development and disease (20). HA accumulates after a myocardial infarction within the interstitial space, which leads to edema (21,22). The presence of fluid within the myocardium also has implications for cardiac electrophysiology, in addition to changing the compliance of the heart wall. A landmark study investigating the role

Submitted October 11, 2018, and accepted for publication February 19, 2019.

*Correspondence: galie@rowan.edu

Editor: Alan Grodzinsky.
https://doi.org/10.1016/j.bpj.2019.02.018

of HA after an infarction found that treatment with hyaluronidase significantly improved ejection fraction (23). However, these in vivo experiments could not determine whether HA primarily acted through matrix or cell-mediated effects. Therefore, the advantage of performing experiments using in vitro models of the myocardium is the ability to parse HA's effect on matrix properties and cellular response. Elucidating the role of HA in the pathological cardiac environment may yield a better understanding of the process of heart failure that can follow myocardial infarction.

In this study, HA was added to 3D constructs of native protein matrices seeded with cocultures of cardiomyocytes and cardiac fibroblasts. Alginate, an anionic polysaccharide that has the same charge density as HA, was used as a control for the matrix effects of HA because it also impedes the transport of fluid out of the matrices, which is resisted by the increased osmotic pressure resulting when the mobile counterions required for charge neutrality are confined to a smaller volume (24). Several testing configurations were used to measure the effect of HA on the cell-mediated contraction of the surrounding matrix, including a tensiometer that measured the force exerted by compacting bulk matrices and micropatterned constructs that were mechanically paced to determine contraction dynamics.

METHODS

Cell-matrix formulation

Cardiomyocytes and cardiac fibroblasts were isolated from the ventricles of euthanized, 1–3-day-old Sprague-Dawley rats. Cells were seeded at a density of 0.75–1 million cells/mL into constructs containing a composite of salmon fibrin (SEA-133; Sea Run Holdings, Freeport, ME), bovine collagen type I (MP Biomedical, Solon, OH), and varying concentrations of high-molecular-weight HA (1690–2100 kDa) derived from *Streptococcus equi* (Sigma, St. Louis, MO). Some constructs also contained sodium alginate (Sigma) to control for the anionic charge of HA. For all conditions, the final concentrations of the fibrin and collagen were 1 and 0.25 mg/mL, respectively, and the HA concentration was 0.5, 1, 2, and 4 mg/mL. Alginate was used at a concentration of 2 mg/mL. To formulate the gels, culture medium (M199 medium supplemented with 10% chick embryo extract and 0.1% antibiotic antimycotic solution (Sigma)) was added to cells along with thrombin (Sigma) (1 unit/mg of fibrinogen), NaOH (Sigma), and 10× phosphate-buffered saline (PBS) (ThermoFisher, Waltham, MA). To initiate polymerization, collagen dissolved in 0.02 M acetic acid (VWR) was added to the solution along with 5 mg/mL fibrinogen (resulting in a final concentration of 1 mg/mL). The mixture was then added to the testing platform (24-well plate for the tensiometer experiments or microTUG substrate) and allowed to polymerize at 37°C.

Rheological experiments

Acellular gels were polymerized on a strain-controlled rheometer fitted with a 20-mm cone-plate (TA Instruments, New Castle, DE). The rheometer applied 1% strain at a frequency of 1 Hz for 4–6 min at room temperature. The gel solution was pipetted on the stage of the rheometer, and measurements were recorded at a sampling rate of 0.2–0.5 Hz. A total of at least three gels for each HA and alginate condition were tested and compared to the collagen-fibrin control.

Tensiometer experiments

A tensiometer (Kibron, Helsinki, Finland) probe described in a previous study to determine force/deformation relationships (25) was used to measure the force of compacting constructs of varying compositions. After adding 1 mL of the cell-gel mixture to the 24-well plate, the sterilized tensiometer probe was inserted into the unpolymerized mixture and lowered into contact with the bottom of the well. A custom polycarbonate cover was placed over the probe to maintain sterility while inside the incubator. The probe was then elevated 1 mm so that 4 mm of the probe length remained inside the mixture. After 1 h at 37°C, 2 mL of culture medium was added on top of the polymerized gel. The force exerted on the tensiometer was then measured over the course of ~15 h. For the acellular control, this process was repeated in the absence of cells.

MicroTUG experiments

MicroTUG substrates were fabricated using soft lithography. A full description of the fabrication can be found in earlier publications (26,27). Briefly, SU-8 photoresist (MicroChem, Westborough, MA) was spun onto silicon wafers, exposed through a photomask, and then etched to create two posts within an array of microwells. The positive-feature silicon master was then silanized before casting negative-feature polydimethylsiloxane (Corning, Corning, NY) stamps. The stamps were plasma treated, silanized, and then used to generate the final substrates. To generate the microtissues, the cell-seeded gel mixture was centrifuged into the Pluronic-treated wells of the microTUG substrates and the excess was aspirated. The substrates were then turned upside down and centrifuged again to position the cell-gel mixture at the heads of the microTUG posts. Microtissues were incubated for 6–7 days, with daily culture medium changes, before indentation with the atomic force microscope (AFM).

The microtissues were stimulated mechanically by indentation with a 3-μm bead fixed to the cantilever of an AFM. Indentations greater than 0.5 μm were sufficient to elicit a coordinated contraction of the constructs within the microTUG substrates, regardless of the location of the probe on the construct. The force exerted by the contracting microtissues was measured by tracking the deflection of the posts, assuming a spring constant of 0.45 μN/μm. The movement of the posts also yielded the dynamics of the contraction, allowing for calculations of time to peak and time to 20 and 80% relaxation. A previous publication detailed the method of using indentation to stimulate cardiac microtissues (28). Alignment of cells within the construct was calculated by taking the dot product of the long axis of the cell with the orientation of the microTUG wells.

Construct immunofluorescence

Constructs were fixed in 4% paraformaldehyde (Alfa Aesar, Haverhill, MA) for 10 min, washed in PBS, and permeabilized in 0.1% Triton X-100 (Sigma) for 20 min before staining. Constructs were incubated for an hour at 37°C with a mixture of Texas Red phalloidin (1:50) (Sigma), 4′,6-diamidino-2-phenylindole (1:1000) (Sigma), and a primary antibody for α-actinin (1:100) (Cell Signaling Tech, Danvers, MA). After washing with PBS, the constructs were incubated for 45 min at 37°C with a secondary antibody conjugated to fluorescein isothiocyanate (1:200). After the tensiometer experiments, a Live/Dead assay (Sigma) was used to measure the viability of cells within the constructs.

Scanning electron microscopy

Acellular constructs were fixed in 4% paraformaldehyde and 2.5% glutaraldehyde (Alfa Aesar) before ethanol dehydration and lyophilized in a critical point dryer (Cryostar NX50; ThermoScientific). Samples were then sputter coated and imaged with a Phenom Pure SEM (Nanoscience

Instruments, Phoenix, AZ). Average fiber diameter was measured in ImageJ using $n = 100$ for each condition.

Statistical analysis

One-way analyses of variance and post hoc Tukey tests were used to test for significance, using a p-value of 0.05. There are at least three samples per condition for all the testing platforms. Two sample t-tests were used to test for statistical significance between individual samples. There are at least three samples per condition for all the testing platforms. Tensiometer data were plotted using 95% confidence intervals.

RESULTS

Addition of HA and alginate alter the viscoelastic properties, but not the storage modulus of fibrin/collagen composite matrices

Rheology was conducted to assess the viscoelastic mechanical properties of the hydrogels before cell seeding. The purpose of this testing was to assess if incorporation of the charged polysaccharides would affect the initial mechanical environment experienced by the cells. Both low-molecular-weight (8 kDa) and high-molecular-weight HA (1.6–2.2 MDa) used in the cell experiments were evaluated. As shown in Fig. 1 *A*, both sizes of HA and alginate affect the rate at which the storage modulus increases. Additionally, the loss angle of the HA- and alginate-containing gels is initially considerably higher than the collagen/fibrin composite gels (Fig. 1 *B*). Quantification of the equilibrium storage modulus indicated that although there was a slight reduction, HA and alginate did not result in any significant difference (Fig. 1 *C*). However, as is evident in the polymerization curves, both the loss angle and the time to polymerization are significantly increased by both sizes of HA and alginate (Fig. 1, *D* and *E*). Furthermore, there is no significant difference between HA and alginate in any of the rheological properties, suggesting that the polysaccharides exert the same effects on the hydrogel viscoelasticity.

Scanning electron microscopy (SEM) was then performed to interrogate the effects of HA and alginate on the microstructure of the collagen-fibrin hydrogels. Collagen-fibrin gels containing HA or alginate appeared opaque after polymerization, suggesting an increased fiber diameter. Analysis of the SEM images validated the increased diameter of the fibers in the presence of HA or alginate (Fig. 2 *A*). The fiber diameter was ~100 nm (Fig. 2 *B*), which is consistent with previous measurements of fibrin (29). Furthermore, the effect of HA on the diameter of fibrin fibers agrees with previous microstructural studies (30).

Constructs containing HA and alginate exert less force during cell-mediated contraction

Cell-seeded constructs polymerized in well plates were constrained from compacting in the radial direction because of attachment at the wall. The fibrin in the matrix of the construct facilitated nonspecific attachment to both the sides of the well and the tensiometer probe. The top surface of the gel was unconstrained and thus able to strain axially as the cells attached and exerted a force on the surrounding matrix. Fig. 3 *A* illustrates the process by which the tensiometer measured the force of this compaction in this configuration. The force was measured over the span of ~15 h.

Fig. 3 *B* shows the effect of adding varying concentrations of HA and alginate to the construct. In the absence of either polysaccharide, the force measured by the tensiometer increased to 0.25 mN by ~10 h after polymerization before reaching a plateau. The addition of either HA or alginate substantially attenuated the force exerted on the probe by the compacting construct. Incorporating 1 mg/mL of HA into the construct reduced the compaction force ~40% to 0.15 mN. Like the non-HA controls, the highest rate of

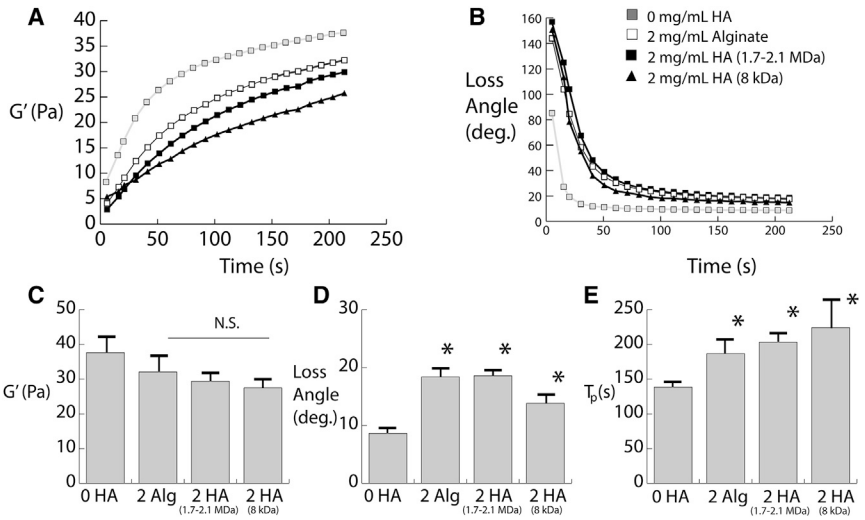

FIGURE 1 (*A*) Storage moduli during gel polymerization. (*B*) The loss angle during polymerization is shown. (*C*) The quantification of storage moduli is shown. (*D*) The quantification of loss angle is shown. (*E*) Time to polymerization (defined as time required to reach 90% of equilibrium loss angle) is shown. *p-value < 0.05. Error bars represent one SD.

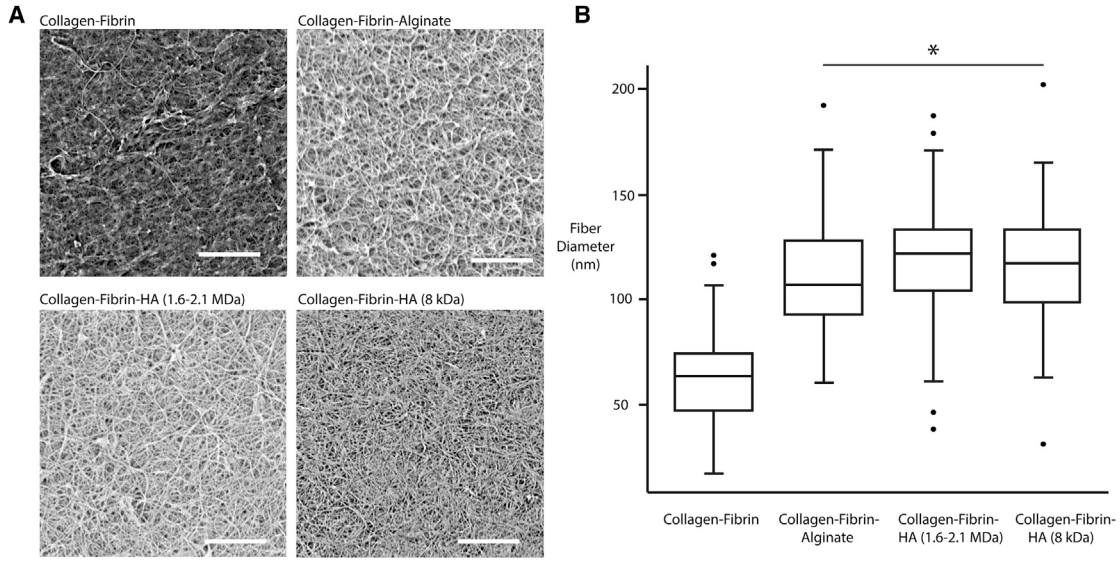

FIGURE 2 (*A*) Scanning electron micrographs of collagen-fibrin 3D scaffolds with and without the addition of hyaluronan (HA) or alginate. Scale bars, 5 μm. (*B*) The quantification of mean fiber diameter is shown. $*p < 0.05$. In the box plot, the error bars represent the minima and maxima of the measured values.

change in the force occurred in the first 10 h after polymerization. The force reduced with HA concentration in a dose-dependent manner: 2 mg/mL of HA reduces the peak force to 0.1 mN, and 4 mg/mL results in a force of nearly 0.05 mN. The addition of alginate also reduced the force measured by the tensiometer. However, the plateau in force observed in the HA-containing constructs was less apparent after the addition of alginate. In the absence of cells, the tensiometer did not measure any change in the force applied by the hydrogel on the probe.

The effect of HA and alginate on cell viability

To assure that adding HA and alginate was not having a cytotoxic effect on the cardiomyocytes and fibroblasts seeded in the matrices, viability assays were conducted after the tensiometer experiments. After the probe was removed, the gel was fixed and removed from the well plate for staining and visualization. As Fig. 4 shows, cells in the non-HA-containing fibrin/collagen composite gels displayed very high viability. Nonviable cells were sparse and scattered throughout the construct. Constructs containing either 4 mg/mL HA or 2 mg/mL alginate showed similar levels of viability. Hence, the effect of HA and alginate on the reduced force was not due to any cytotoxic effects or masking of adhesion sites but rather a change in either the matrix mechanical properties or actomyosin contractility of the seeded cells.

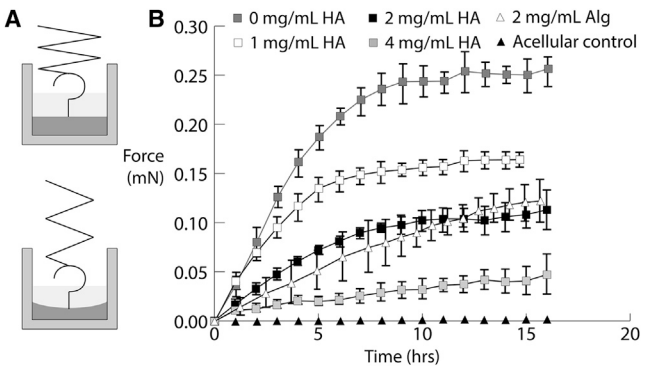

FIGURE 3 (*A*) Schematic of the tensiometer testing setup: the cell-seeded construct is polymerized within a well plate with the probe inserted near the center. Compaction can only occur in the axial direction because of the radial constraints of the well plate. (*B*) Force measurements for constructs containing varying levels of HA and 2 mg/mL alginate over a span of ~15 h is shown. Error bars represent one SD.

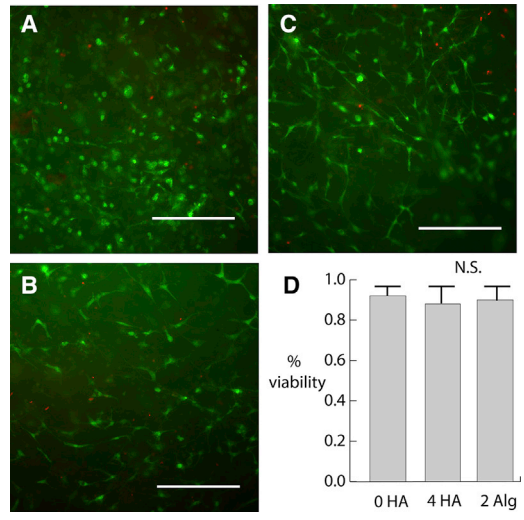

FIGURE 4 (*A*) Live/Dead assay on a 0 mg/mL HA hydrogel removed from the Kibron probe after 24 h of testing. (*B*) 4 mg/mL HA and (*C*) 2 mg/mL alginate are shown. Scale bars, 300 μm. (*D*) Quantification of viability, error bars represent one SD. To see this figure in color, go online.

Microtissues containing HA and alginate exhibited altered contraction dynamics in the microTUG system

To elucidate how HA alters the dynamics of cell-mediated contraction, cells were seeded in the microTUG system. When stimulated by an AFM tip, constructs within microTUG substrates undergo a coordinated contraction, which mimics the contraction of the myocardium during systole in vivo. A previous study characterized this mechanical stimulation of the microtissues and demonstrated that continuous indentation at ~1 Hz was required to maintain beating of the construct (28). This setup provided an alternate means to study force generation for comparison with the tensiometer data. Moreover, use of the microTUG system allowed for a more detailed observation of the dynamics of cell-mediated contraction of the matrix. Whereas the force profile measured by the tensiometer occurred over the span of hours and involved both myocytes and fibroblasts, the contraction in the microTUG system lasted for ~1 s and was primarily driven by myocytes.

Fig. 5 *A* shows a bright-field image of a cell-seeded construct within one well of a microTUG substrate. The image shows the tissue fixed to the posts within the well, as well as the location of the AFM cantilever (*black triangle*). The indentation was performed near the centerline of the construct for each condition. Fig. 5 *B* shows the averaged force profiles of the constructs during mechanically induced contraction. Constructs without HA or alginate exerted the highest force on the microTUG posts, with a peak of ~5 μN. Similar to the tensiometer experiments, incorporating HA reduced the force exerted by the cell-seeded construct. The addition of 1 mg/mL HA reduced the peak force to 3 μN, and 2 mg/mL of HA or alginate further attenuated the force to ~2 μN. Again, there was no significant difference between the effects of HA and alginate on force generation of the constructs.

The dynamics of the contraction events were also affected by the presence of HA and alginate. In the absence of either polysaccharide, the contraction event lasted less than 1 s. Fig. 5 *C* indicates that the time to peak is significantly higher using constructs containing 2 mg/mL HA or alginate. Fig. 5, *D* and *E* show that the relaxation time, quantified by the time required to relax to 20 and 80% of the peak force, was also significantly elevated by the presence of HA and alginate. There was no significant difference in any of the time to peak or relaxation quantities between constructs containing HA and alginate. Both polysaccharides significantly extended the period of the contraction, and their force profiles were symmetric between shortening and relaxation. Considering that alginate does not have any biochemical effect on the cells within the construct, these results suggest that the effect of HA was due primarily to its water- and counterion-sequestering properties within the matrix. By impeding fluid from exiting the matrix, HA attenuated the observed force and rate of cell-mediated contraction.

HA and alginate disrupt self-organization of cardiac microtissues

Cardiomyocytes and fibroblasts seeded within microtissues self-assembled into a structure resembling myofibrils in vivo. Cardiomyocytes aggregated and oriented parallel to the centerline of the tissue, and fibroblasts attached around the outer perimeter of this central myofibril. This

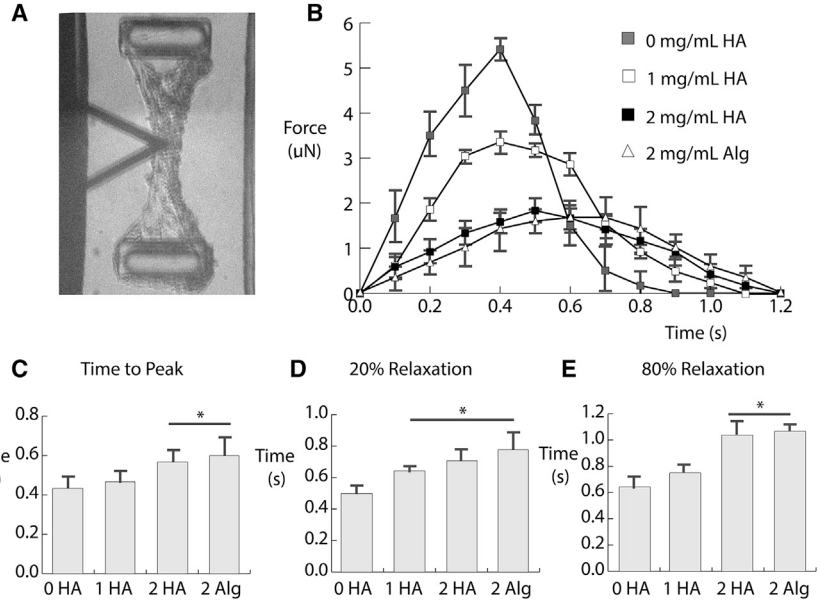

FIGURE 5 (*A*) Bright-field image of the microTUGs being stimulated by an AFM tip. (*B*) The force exerted by the constructs on the microTUG posts during a contraction event is shown. Each condition is the average force produced by at least $n = 3$ samples over the period of a contraction. The dynamics of the different matrix formulations, including (*C*) time to peak, (*D*) 20% relaxation, and (*E*) 80% relaxation are shown. Error bars represent one SD.

structure was most apparent in Fig. 6, *A* and *B*, which represent 0 and 1 mg/mL HA, respectively. The tissues were stained with phalloidin to illuminate F-actin and with anti-α-actinin, which localizes to the z-disks of sarcomeres within the neonatal myocytes. Cardiomyocytes were distinguished by a striated, positive stain for α-actinin. In contrast, fibroblasts (denoted by *white arrows* in Fig. 6, *C* and *D*) only stained positive for the phalloidin. The addition of higher concentrations of HA and alginate resulted in increased tissue diameter and reduced alignment of the cardiomyocytes, as shown in Fig. 6, *C* and *D*. There was no separation between myocytes and fibroblasts, and the inner core of cardiomyocytes along the centerline of the tissue was not present.

Fig. 6, *C* and *D* show how the polysaccharides altered the structure and the self-assembly of the myofibrils within the constructs. 2 mg/mL of HA and alginate significantly increased the resting diameter of the microtissues within the microTUG substrates. This result suggests that the cellular organization observed without HA or alginate involved compaction of the surrounding matrix. It is unclear whether the reduced compaction is due to an inability of the cells to properly compact the matrices around the microTUG posts or a direct effect on cell function or geometry. Quantification of the misalignment induced by HA and alginate in Fig. 6 *D* verified that their presence disrupted the self-assembly of the cardiomyocytes. This misalignment likely contributed to the reduction in force during the mechanically stimulated contractions shown in Fig. 5.

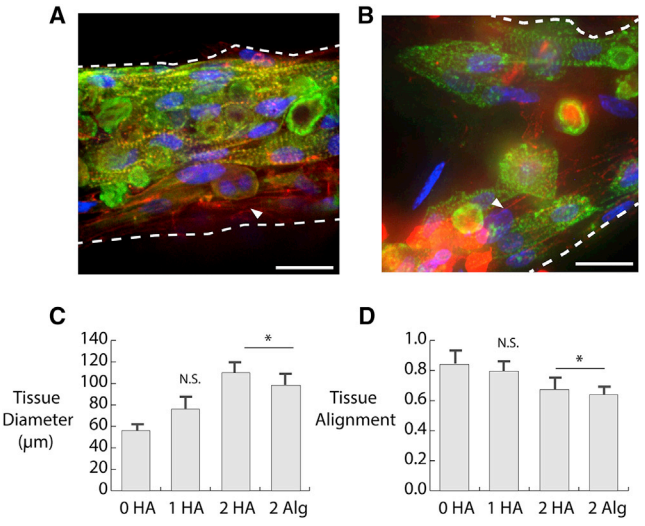

FIGURE 6 Immunofluorescence images of microTUG constructs stained for α-actinin (*green*), phalloidin (*red*), and 4′,6-diamidino-2-phenylindole (*blue*) for (*A*) 0 mg/mL HA and (*B*) 1 mg/mL HA. White arrows show fibroblasts on the perimeter of the construct. Scale bars, 20 μm. The white arrow denotes the location of fibroblasts within the microtissues. (*C*) The construct diameter is measured at the middle of the microtissue portrayed in the bright-field images in Fig. 2 *A*. (*D*) Tissue alignment is measured by taking the dot product between the long axis of the cells and the construct. Error bars represent one SD. To see this figure in color, go online.

DISCUSSION

In this study, we aimed to bridge the gap between the effect of HA in vivo, where it is upregulated in the myocardium after injury (31), and its impact on cardiomyocytes in vitro, where it induces a hypertrophic-like effect when incorporated in two-dimensional (2D) substrates (13). To provide a closer approximation of the in vivo microenvironment using an in vitro setting, fibrin-based 3D hydrogels were seeded with a coculture of cardiac fibroblasts and cardiomyocytes isolated from the ventricles of neonatal rat hearts. Varying amounts of HA were added to the hydrogel to assess its impact on both the matrix properties and cell response. Alginate, which shares a similar chemical structure to HA without directly activating cell-surface receptors, was used as a control to distinguish between the cell and matrix effects of HA. The force exerted by cells within the hydrogels was assessed using two testing methods: a tensiometer that measured the passive force exerted by the cell-seeded hydrogels over a period of 15–24 h and a microfabricated tissue gauge that quantified the force applied by stimulated cardiomyocytes within the constructs after a week in culture.

Both testing platforms indicated that HA reduced the tension generated by cardiac cells on their surrounding matrix. However, the modification of the physical-chemical properties of the matrix appeared to be the dominant effect of HA because alginate exhibited a similar effect during both passive contraction in the tensiometer experiments and active contraction in the microTUG platform. A change in fibroblast/cardiomyocyte ratio was likely not the cause of the reduced force because the tensiometer and microTUG experiments yielded similar results despite their substantially different time frames. The result that neither HA nor alginate had any significant effect on the storage modulus of the collagen/fibrin hydrogels suggested that the cell response was also not due to any initial difference in substrate stiffness. Given that the polysaccharides both increased the viscoelastic properties of the hydrogel, as evidenced by an increased loss angle and structural differences in the hydrogel microstructure, it is possible that the increase in viscous loss caused by HA and alginate resulted in the observed reduction of cell-matrix tension. A recent study reported a similar finding by demonstrating that increasing the viscous loss of a 2D viscoelastic substrate caused a reduction in spread area and cell stiffness (32).

Alternatively, one difference between the 2D and 3D environments is that cell-matrix tension results in a reduction of volume in the 3D hydrogels. Therefore, an additional explanation for the effects of HA and alginate is the ability of these polymers to sequester counterions within the

hydrogel, creating an osmotic pressure gradient that resists the volume change caused by contraction of the embedded cells. Assuming that all of the anionic carboxyl groups on each disaccharide unit are associated with potassium or sodium ions, the matrix would contain an ~6-mM counterion concentration. Using the van 't Hoff equation, $\Pi = iMRT$, this concentration translates to 13.6 kPa of osmotic pressure. To determine if this osmotic pressure can account for the difference in volume change between hydrogels with and without HA and alginate, we calculated the pressure difference caused by concentrating the counterions in a smaller volume and compared this pressure with the bulk modulus of the hydrogel (K is ~600 Pa based on previous measurements of shear modulus and an assumed Poisson's ratio of 0.35). Assuming linear volumetric strain,

$$\Delta P = -K\frac{\Delta V}{V},$$

and using values from the tensiometer experiments shown in Fig. 3, this equation estimates a pressure difference of 60 Pa, which is several orders of magnitude less than the estimated osmotic pressure. However, because it is likely that not all disaccharide units in the polymer are ionized, this overestimation is expected. A previous analysis of the polyelectrolyte properties of HA support the assumption that ionization of the disaccharide units at the concentrations used in this study is limited (33). Therefore, this calculation demonstrates that the osmotic effects of HA and alginate can account for the inability of these gels to contract volumetrically. This analysis suggests that future studies into the biochemical effects of HA should employ constrained 3D environments, which has been done recently in a 3D astrocyte study (34).

Overall, this study provides insight into the substantial impact that HA has on tissues like the myocardium. In the models tested here, the physical properties of HA superseded any direct biochemical effects on the cell response. However, as detailed in the preceding paragraph, the use of hydrogels that undergo a decrease in volume may accentuate the physical-chemical effects of HA and mask its biochemical effects. Nonetheless, although compacting hydrogels do not mimic any specific process in vivo, the fibrotic scar that develops after myocardial infarction does undergo substantial volume change during the progression of heart failure (35,36). Therefore, the effect of HA on the viscoelastic properties of the matrix should be recognized in addition to its established effects on matrix organization. Finally, the results of this study may also be useful for the design of new biomaterials and regenerative therapies that can benefit from the physical-chemical effects of HA. For example, cardiac patches are increasing in complexity and effectiveness; using a material like HA may protect the structure and integrity of the patch after delivery.

AUTHOR CONTRIBUTIONS

N.B., P.A.G., and P.A.J. designed research. N.B. and P.A.G. performed research. N.B., P.A.G., and P.A.J. analyzed data and wrote the manuscript.

ACKNOWLEDGMENTS

This study was supported by grants provided from the American Heart Association and National Science Foundation to P.A.G. and grant EB017753 (P.A.J. and P.A.G.) from the National Institutes of Health.

REFERENCES

1. Chrzanowska-Wodnicka, M., and K. Burridge. 1996. Rho-stimulated contractility drives the formation of stress fibers and focal adhesions. *J. Cell Biol.* 133:1403–1415.
2. Bhadriraju, K., M. Yang, …, C. S. Chen. 2007. Activation of ROCK by RhoA is regulated by cell adhesion, shape, and cytoskeletal tension. *Exp. Cell Res.* 313:3616–3623.
3. Nelson, C. M., D. M. Pirone, …, C. S. Chen. 2004. Vascular endothelial-cadherin regulates cytoskeletal tension, cell spreading, and focal adhesions by stimulating RhoA. *Mol. Biol. Cell.* 15:2943–2953.
4. Assoian, R. K., and E. A. Klein. 2008. Growth control by intracellular tension and extracellular stiffness. *Trends Cell Biol.* 18:347–352.
5. Giannone, G., and M. P. Sheetz. 2006. Substrate rigidity and force define form through tyrosine phosphatase and kinase pathways. *Trends Cell Biol.* 16:213–223.
6. Halder, G., S. Dupont, and S. Piccolo. 2012. Transduction of mechanical and cytoskeletal cues by YAP and TAZ. *Nat. Rev. Mol. Cell Biol.* 13:591–600.
7. Dupont, S., L. Morsut, …, S. Piccolo. 2011. Role of YAP/TAZ in mechanotransduction. *Nature.* 474:179–183.
8. Janmey, P. A., R. G. Wells, …, C. A. McCulloch. 2013. From tissue mechanics to transcription factors. *Differentiation.* 86:112–120.
9. Cui, Y., F. M. Hameed, …, M. Sheetz. 2015. Cyclic stretching of soft substrates induces spreading and growth. *Nat. Commun.* 6:6333.
10. Galie, P. A., A. van Oosten, …, P. A. Janmey. 2015. Application of multiple levels of fluid shear stress to endothelial cells plated on polyacrylamide gels. *Lab Chip.* 15:1205–1212.
11. Engler, A., L. Bacakova, …, D. Discher. 2004. Substrate compliance versus ligand density in cell on gel responses. *Biophys. J.* 86:617–628.
12. Yeung, T., P. C. Georges, …, P. A. Janmey. 2005. Effects of substrate stiffness on cell morphology, cytoskeletal structure, and adhesion. *Cell Motil. Cytoskeleton.* 60:24–34.
13. Chopra, A., M. E. Murray, …, P. A. Janmey. 2014. Augmentation of integrin-mediated mechanotransduction by hyaluronic acid. *Biomaterials.* 35:71–82.
14. Hellström, M., B. Johansson, and A. Engström-Laurent. 2006. Hyaluronan and its receptor CD44 in the heart of newborn and adult rats. *Anat. Rec. A Discov. Mol. Cell. Evol. Biol.* 288:587–592.
15. Laurent, T. C., U. B. Laurent, and J. R. Fraser. 1996. The structure and function of hyaluronan: an overview. *Immunol. Cell Biol.* 74:A1–A7.
16. Nakamura, M., and T. Nishida. 1999. Synergistic effects of hyaluronan and fibronectin on epithelial migration in rabbit cornea in vitro. *Cornea.* 18:686–692.
17. Oliferenko, S., I. Kaverina, …, L. A. Huber. 2000. Hyaluronic acid (HA) binding to CD44 activates Rac1 and induces lamellipodia outgrowth. *J. Cell Biol.* 148:1159–1164.
18. Turley, E. A., L. Austen, …, K. Hoare. 1993. Ras-transformed cells express both CD44 and RHAMM hyaluronan receptors: only RHAMM is essential for hyaluronan-promoted locomotion. *Exp. Cell Res.* 207:277–282.

19. McCourt, P. A., B. Ek, …, S. Gustafson. 1994. Intercellular adhesion molecule-1 is a cell surface receptor for hyaluronan. *J. Biol. Chem.* 269:30081–30084.

20. Gerdin, B., and R. Hällgren. 1997. Dynamic role of hyaluronan (HYA) in connective tissue activation and inflammation. *J. Intern. Med.* 242:49–55.

21. Waldenström, A., H. J. Martinussen, …, R. Hällgren. 1991. Accumulation of hyaluronan and tissue edema in experimental myocardial infarction. *J. Clin. Invest.* 88:1622–1628.

22. Hällgren, R., B. Gerdin, …, G. Tufveson. 1990. Accumulation of hyaluronan (hyaluronic acid) in myocardial interstitial tissue parallels development of transplantation edema in heart allografts in rats. *J. Clin. Invest.* 85:668–673.

23. Kresh, J. Y., H. F. Frasch, …, S. K. Brockman. 1997. Intramyocardial regulation of coronary dynamics. *In* Cardiac-Vascular Remodeling and Functional Interaction. Y. Maruyama, M. Hori, and J. S. Janicki, eds. Springer, pp. 295–307.

24. McLane, L. T., P. Chang, …, J. E. Curtis. 2013. Spatial organization and mechanical properties of the pericellular matrix on chondrocytes. *Biophys. J.* 104:986–996.

25. Levental, I., P. A. Janmey, and A. Cēbers. 2008. Electrostatic contribution to the surface pressure of charged monolayers containing polyphosphoinositides. *Biophys. J.* 95:1199–1205.

26. Boudou, T., W. R. Legant, …, C. S. Chen. 2012. A microfabricated platform to measure and manipulate the mechanics of engineered cardiac microtissues. *Tissue Eng. Part A.* 18:910–919.

27. Legant, W. R., A. Pathak, …, C. S. Chen. 2009. Microfabricated tissue gauges to measure and manipulate forces from 3D microtissues. *Proc. Natl. Acad. Sci. USA.* 106:10097–10102.

28. Galie, P. A., F. J. Byfield, …, P. A. Janmey. 2015. Mechanically stimulated contraction of engineered cardiac constructs using a microcantilever. *IEEE Trans. Biomed. Eng.* 62:438–442.

29. Yeromonahos, C., B. Polack, and F. Caton. 2010. Nanostructure of the fibrin clot. *Biophys. J.* 99:2018–2027.

30. Hayen, W., M. Goebeler, …, V. Nehls. 1999. Hyaluronan stimulates tumor cell migration by modulating the fibrin fiber architecture. *J. Cell Sci.* 112:2241–2251.

31. Matsushita, T., M. Oyamada, …, T. Takamatsu. 1999. Remodeling of cell-cell and cell-extracellular matrix interactions at the border zone of rat myocardial infarcts. *Circ. Res.* 85:1046–1055.

32. Charrier, E. E., K. Pogoda, …, P. A. Janmey. 2018. Control of cell morphology and differentiation by substrates with independently tunable elasticity and viscous dissipation. *Nat. Commun.* 9:449.

33. Cleland, R. L., J. L. Wang, and D. M. Detweiler. 1982. Polyelectrolyte properties of sodium hyaluronate. 2. Potentiometric titration of hyaluronic acid. *Macromolecules.* 15:386–395.

34. Bowers, H. C., M. L. Fiori, …, P. A. Galie. 2019. Cell-matrix tension contributes to hypoxia in astrocyte-seeded viscoelastic hydrogels composed of collagen and hyaluronan. *Exp. Cell Res.* 376:49–57.

35. Ursell, P. C., P. I. Gardner, …, A. L. Wit. 1985. Structural and electrophysiological changes in the epicardial border zone of canine myocardial infarcts during infarct healing. *Circ. Res.* 56:436–451.

36. Sutton, M. G., and N. Sharpe. 2000. Left ventricular remodeling after myocardial infarction: pathophysiology and therapy. *Circulation.* 101:2981–2988.